

Temperature Dependence of Electron and Hole Signals in Irradiated $p^+ - n - n^+$ Diodes in the Presence of Continuous Carrier Injection

Marko Zavrtanik, Vladimir Cindro, Gregor Kramberger, Igor Mandič and Marko Mikuž

Abstract—The temperature dependence of electron and hole signals in irradiated $p^+ - n - n^+$ diodes was studied in the presence of carrier injection. Diodes fabricated on high (15 k Ω cm) resistivity silicon wafers were irradiated with neutrons up to a 1MeV-neutron equivalent fluence of $2 \times 10^{14}/\text{cm}^2$. The detector signal after illumination with a fast (FWHM \sim 1ns) red ($\lambda = 670$ nm) light pulse was amplified with a fast amplifier ($f_t = 1\text{GHz}$) and recorded with a fast digitizing oscilloscope. During measurements the electron or hole densities were changed by illuminating the detector with light of short penetration depth. The effect of charge trapping was studied by observing the change in effective space charge density as the flux of injected carriers was varied. The effect of continuous carrier injection on signal decay at cryogenic temperatures was also observed.

I. INTRODUCTION

SILICON detectors with their excellent spatial resolution, signal to noise ratio, fast read out and low radiation length seem to be the technical solution to be used for tracking purposes in the majority of present and future HEP experiments. However an extremely harsh radiation environment is to be expected for the tracking systems of future experiments such as the ones at the Large Hadron Collider where significant detector performance deterioration due to high hadronic radiation fluences will occur. The radiation hardness of these devices is therefore of extreme importance. This fact resulted in an impressive number of systematic studies covering microscopic as well as macroscopic effects.

Our study is focused on the effect of photo-generated electrons or holes on the performance of strongly irradiated detectors where deep level defects exceed the shallow dopant density. This modus operandi was theoretically [1], [2] and practically [3] considered by other groups, but left experimentally only partially exploited.

In our work we show that electric field engineering by charging of defects is possible and practical. Charging can be achieved by providing a surface generated current, increasing in that way the density of either electrons or holes. An optically accessible current signal measuring set-up was

implemented to demonstrate this. The shape of the current signal resulting from electron-hole pairs created in the active region was measured at the contacts of a Si detector. Its shape depends on the electric field strength in the device. If the electrical transfer function of the measurement system is known and accounted for, a number of device parameters can be deduced by measuring the current pulse [3]. This technique, which originates in the early seventies, is nowadays often called the Transient Current Technique (TCT). Electron-hole pairs are created by means of a short laser pulse. The spatial distribution of the pairs depends on the absorption constant α , which in turn is inversely related to the wavelength. If red light is used, the majority of electron-hole pairs are created in the close proximity of the device surface, since $\alpha^{-1} = 3.3 \mu\text{m}$ for $\lambda = 670$ nm at room temperature [4]. Creation of such a group in the direct vicinity of a negatively or positively biased contact forces electrons or holes, respectively, to travel through the whole of the detector while the other charge carriers are collected immediately by the adjacent electrode. This gives the possibility to distinguish between the electron and hole signals. To study defect charging an additional source of light is needed to generate a continuous flux of electrons or holes in the sample. Transient current signals, acquired in the presence of an increased density of electrons or holes, provide information about the effect of trap filling on the electric field development.

II. THE EXPERIMENTAL PARAMETERS

A. The Experimental Set-up

The experimental set-up was built around a Janis VPF-100 LN2 pour fill optical cryostat which allowed the temperature to be varied between 77 K and 300 K with 0.2 K stability. The electrical connection between the sample mounted inside the cryostat and the rest of the read-out system was made by means of a single semi-rigid micro coaxial cable. A Picosecond PulseLab 5532 Bias-T was used to supply reverse bias to the sample. The Keithley 2001 IV meter which was used for this purpose allows simultaneous monitoring of the current driven through the device under test. The electron-hole pairs were created using a Toshiba TOLD9221M visible laser diode ($\lambda = 670$ nm) driven with six parallel advanced

Manuscript received November 5, 2000.

Corresponding author: Marko Zavrtanik, Jožef Stefan Institute, Jamova 39, SI-1001 Ljubljana, Slovenia (telephone: ++386 1 477 3654, e-mail: marko.zavrtanik@ijs.si)

high-speed CMOS Schmitt trigger inverters (SN54AHC14). The resulting light pulse had a width of 1.4 ns FWHM. Before hitting the sample the light was attenuated and focused to a spot with minimum dimensions of $\sim 100 \mu\text{m}$. The maximum number of electron-hole pairs created by a single laser pulse was 5×10^5 . This number was determined using average power measurement and verified by comparing the results with the spectra obtained when using electrons from a ^{90}Sr source and alpha particles from an ^{241}Am source. Continuous carrier injection was achieved using He-Ne laser ($P_{\text{max}} = 4 \text{ mW}$, $\lambda = 633 \text{ nm}$). By measuring the current driven through the device under test the concentrations of injected electrons or holes were determined as is discussed later. Experimental set-up gave the possibility of independent continuous and pulsed illumination from either side of the detector. Signals were amplified with an MITEQ AM-1309 wide band amplifier (0.01-1GHz, 55 dB) and subsequently digitized with a Tektronix TDS 754 C digital scope. The charge collection efficiency (CCE) was determined using numerical integration in data post processing.

B. The Samples

In this study several p^+-n-n^+ pad detectors produced by ST Microelectronics on high resistivity (15 k Ωcm) standard $\langle 111 \rangle$ silicon wafers were irradiated with neutrons to fluences up to $\phi_{\text{eq}} = 2 \times 10^{14} / \text{cm}^2$ 1 MeV neutron NIEL equivalent. The diodes listed in Table I had a hole ($f = 2 \text{ mm}$) in the metallization on the p^+ side for light injection, while on the n^+ side a mesh metallization was used for the same purpose. The active region of the diodes used was (5 x 5) mm^2 . During and after the irradiation the diodes were kept unbiased. After the irradiation they were annealed at room temperature (RT) to the minimum in full depletion voltage (FDV) and then stored at $T = -17^\circ \text{C}$.

TABLE I
THE SAMPLES USED IN THIS STUDY. FDV WERE MEASURED BY THE CV METHOD AT A FREQUENCY $\nu = 10 \text{ kHz}$ AND $T = 20^\circ \text{C}$

Sample label	$\phi_{\text{eq}} [10^{13} \text{ n/cm}^2]$	FDV in minimum
W3391	5.0	70
W33911	7.5	120
W3392	10.0	160
W3394	20.0	290

III. RESULTS

The TCT measurements were performed on all of the samples. For the sake of clarity the majority of the results presented correspond to the sample W3391. Fig 5 however summarizes the results obtained with all of the samples.

A. Space Charge Inversion

An example of the bias voltage dependence of laser-induced electron signals for a detector irradiated to $\phi_{\text{eq}} = 5 \times 10^{13} \text{ n/cm}^2$ at $T = -10^\circ \text{C}$ is shown in Fig. 1. The shape of

the electron signals indicates type inversion ($n \rightarrow p$) has occurred so that the highest field is at the n^+ contact. It can also be observed that only a small current is induced at low bias voltages due to electrons being injected in the low field region.

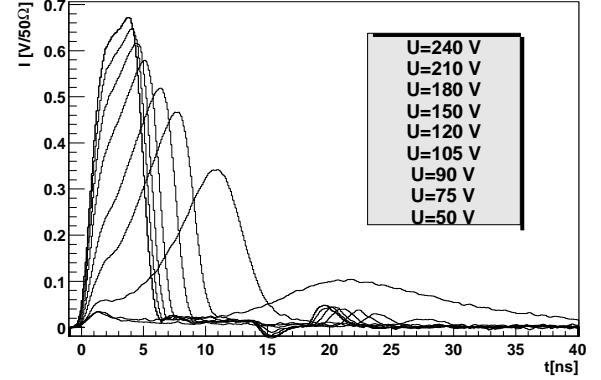


Fig. 1. Bias voltage dependence of electron signal (p^+ side illumination)

Degraded charge collection can be even better observed by looking at electron signal charge collection as a function of bias voltage (Fig. 2 a, solid squares). A region of low field injection is followed by a steep increase in efficiency as the FDV is approached. This predictable situation is dramatically changed if additional electrons or holes are injected in the continuous (DC) mode. The effect of DC electron injection is shown in Fig. 2 a (open circles).

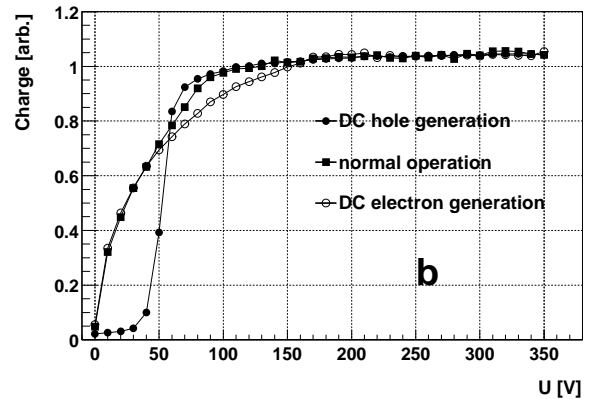
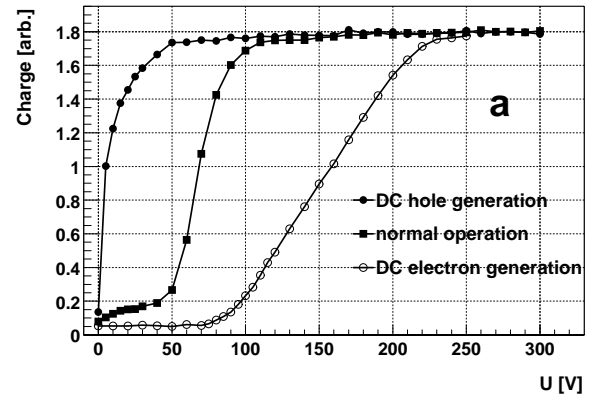


Fig. 2. Charge collection versus bias voltage for electron (a) and hole (b) signals in sample W3391. The y-axis unit corresponds to 3×10^5 e-h pairs.

Comparison with data taken with no DC charge injected clearly shows that FDV is increased and that full charge collection is reached at higher bias voltages. An opposite effect, however, can be observed in the case of DC hole injection (rear side DC illumination). FDV decreases and saturated charge collection is reached at much smaller bias voltages, as exhibited in Fig. 2 a (solid circles). Moreover, the absence of a low field injection region indicates that type re-inversion from p^+-p-n^+ back to p^+-n-n^+ is taking place.

Similar conclusions can be deduced from Fig. 2 b where hole signal charge collection dependence on bias voltage is presented. Again a decrease in FDV can be observed in the presence of continuous hole injection. Low field injection at low biases clearly indicates type re-inversion.

This assumption is supported by comparing hole signal shapes acquired in the presence of different levels of hole injection. In Fig. 3 it can clearly be observed that as the injection level increases the signal shape changes from the one characteristic for a p^+-p-n^+ device to the one typically observed in p^+-n-n^+ .

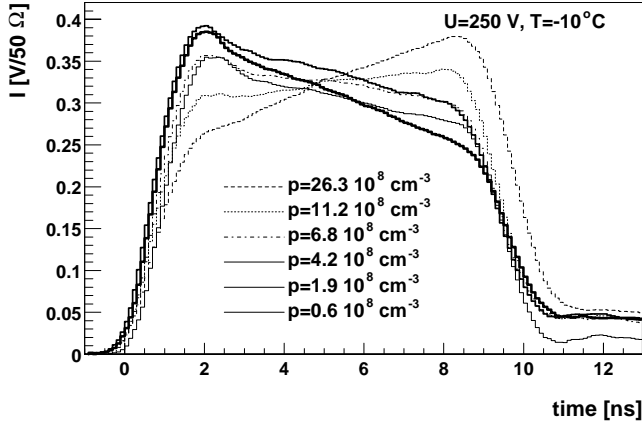


Fig. 3. Comparison of the hole signal shapes measured in the presence of different hole concentrations induced by the continuous illumination of the W3391 sample ($\phi_{eq} = 5 \times 10^{13} \text{ n/cm}^2$, $T = -10^\circ\text{C}$, $U_b = 250\text{V}$).

The injected hole concentrations given in Fig. 3 were determined by measuring the increase in the current driven through the detector when illuminated with the continuous laser beam. From the equation for current density ($j = e_0 p_{nq} v$) it follows:

$$n_{nq} (= p_{nq}) = \frac{\Delta I}{e_0 S v} \quad (1)$$

where p_{nq} , n_{nq} is the injected carrier concentration, ΔI is the increase in current, S is the illuminated area, v is the average velocity of carriers and e_0 is the unit charge. A direct TCT measurement of the time needed for the hole or electron to travel over the whole detector thickness at a given bias voltage determines the average drift velocity of the charge carrier. The average concentration of injected carriers is therefore deduced by means of the current increase and TCT signal shape.

One must however bear in mind that there are two general parameters determining the injected carrier concentration of

positive or negative type. The first is the surface generation rate, governed by the light intensity. The second parameter is the bias voltage or the electric field strength in the sample. As the bias voltage increases the drift velocity of the carriers increases as well. In the case of a constant surface generation rate this results in a decrease of the carrier concentration as less and less time is needed for the carrier to reach the other side of the sample. This parameter affects the concentration during the voltage scan and has to be accounted for.

B. Injected charge trapping

The concentration of free injected holes, ranging between $(0.2 - 1.6) \times 10^9 \text{ cm}^{-3}$, is far from being sufficient to cause a significant change in space charge. Trapping of free carriers has therefore to occur to compensate for the charge of ionized deep level defects. One way to study the effect of trapping is to observe the dependence of the effective space charge (N_{eff}) on the concentration of injected carriers. To do that, N_{eff} was estimated from the fit to the measured induced current shape [5]. To make an estimation of N_{eff} , the trapping probability for electrons and holes has to be deduced. We used the charge correction method, described in [6], to determine the trapping probability from the time evolution of the induced current at biases above the full depletion voltage.

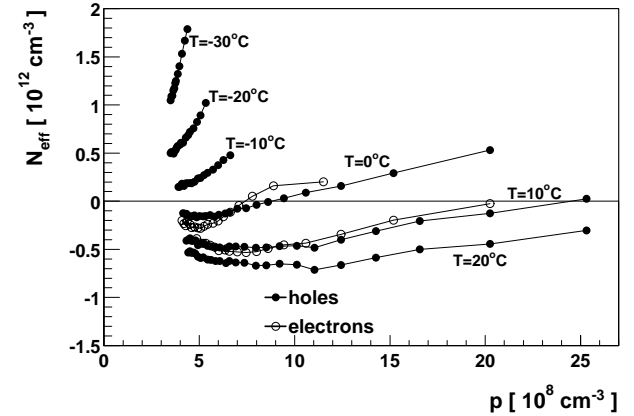


Fig. 4. Dependence of the effective space charge density on the nonequilibrium hole density at different temperatures for W3391 sample ($\phi_{eq} = 5 \times 10^{13} \text{ n/cm}^2$).

In Fig. 4 the dependence of N_{eff} on the injected hole density is presented at different temperatures. The illumination level was held constant during this set of measurements. The change in hole concentration is therefore caused by the variation of the bias voltage. The continuous surface generation rate, inducing a current density of $\Delta I/S = 220 \mu\text{A/cm}^2$, failed to cause type re-inversion at room temperature ($T = 20^\circ\text{C}$). However, when the temperature is lowered the detrapping time becomes longer, resulting in type re-inversion as is the case at $T = 10^\circ\text{C}$ and $T = 0^\circ\text{C}$. At these two temperatures the minimal FDV can be reached with the surface generation rate used in this particular set of measurements. Further reduction of the temperature extends the detrapping time affecting the reemission of the injected

carriers from the deep traps and causing in this way overcompensation of N_{eff} . To reach the optimum working point (minimum FDV) at temperatures $T=-10^\circ\text{C}$, $T=-20^\circ\text{C}$ and $T=-30^\circ\text{C}$ the surface generation rate would have to be reduced.

From Fig. 4 it can therefore be deduced that by carefully choosing the surface generation rate and working temperature N_{eff} can be minimized. In this way optimal operating conditions are reached.

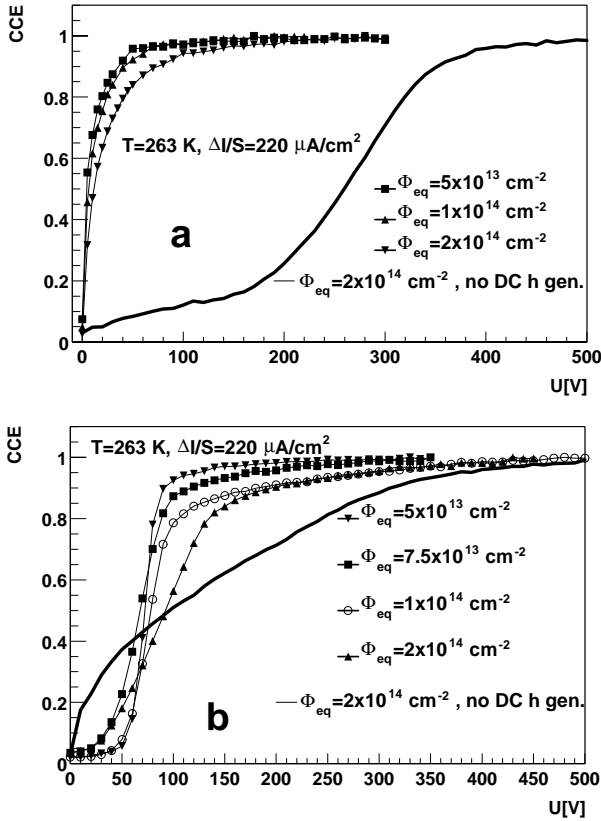


Fig. 5. Charge collection efficiency for a) electron signal and b) hole signal at optimal working point for samples irradiated with fluences from $\Phi_{\text{eq}}=5 \times 10^{13} \text{ n/cm}^2$ to $\Phi_{\text{eq}}=2 \times 10^{14} \text{ n/cm}^2$. Operation without continuous hole injection is represented by a thick line. The plots are normalized to the same terminal CCE at all fluences.

In Fig. 5 one can see that once the optimal temperature and hole concentration is reached, the change in FDV as a function of irradiation fluence is surprisingly small. All of the samples experienced a substantial decrease in FDV which gives the possibility of practical application in set-up where continuous hole injection by surface illumination is feasible.

One must however note that the additional current flowing through the detector in the presence of continuous hole injection increases the shot-noise of a detector-preamplifier combination. Its contribution to the total noise is proportional to square root of integration time and leakage current. Assuming the integration time of 25 ns (CR-RC shaping circuit) and operational temperature around -10°C the contribution to the total equivalent noise charge of a detector with surface S would be 2500 e multiplied by $(S/S_0)^{(1/2)}$

where S_0 is 1 cm^2 . For a typical strip used in some of the LHC experiments ($S= (5 \times 10^{-3} \times 6) \text{ cm}^2$) this results in additional ~ 450 electrons of non correlated noise which has to be summed in square to the other noise contributions typically in the order of 1000 electrons. On the other hand at the optimal operating conditions ($N_{\text{eff}} \sim 0$) the electric field can be established in the whole thickness of detector even at higher detector thickness (for example 1.5 mm). Hence, the increase of noise can be compensated by the increase in signal height.

C. Cryogenic operation

Below $T = -50^\circ\text{C}$ application of the above mentioned measurements and analysis methods becomes problematic. The main reason is the increased mobility of the charge carriers which causes the TCT signals to become short in time in this way approaching the frequency limitations of the measuring system. Once the TCT signal becomes affected by the length of the laser pulse, the determination of the effective space charge and trapping time by the above mentioned methods becomes unreliable. However some basic observations and conclusions can still be deduced from the cryogenic measurements.

The first effect observed is instability of the TCT signal i.e. the signal height decays and its shape changes with the time of measurement [7]. In Fig. 6 the time evolution of the CCE is shown for electron (p^+ side illumination) and hole (n^+ side illumination) signals at two different bias voltages. The time is measured from the time of starting the laser pulses with a certain repetition rate (typical 1 Hz).

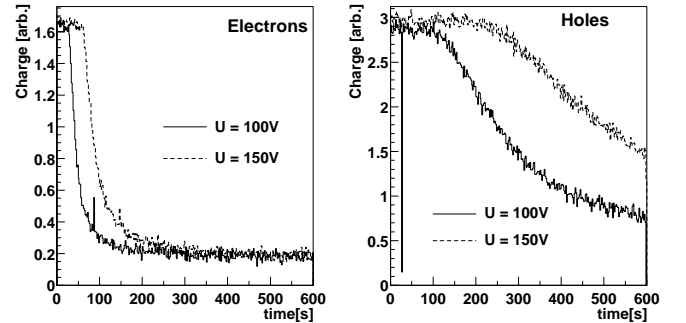


Fig. 6. Time dependence of CCE for electron and hole signals in sample W3394 ($\Phi_{\text{eq}}=2 \times 10^{14} \text{ n/cm}^2$, $T=83 \text{ K}$).

This effect can be explained by trapping of the charge induced by the laser light. Due to the very long detrapping times at low temperatures this trapped charge changes the space charge so that the diode ceases to be fully depleted. In addition, the sign of the trapped charge is such that the junction is always moving away from the light injection side i.e. measuring with electrons the diode bulk becomes of p type whereas with holes the trapped charge is positive and thus the diode becomes of n type.

The rate at which the TCT signal decays is a function of bias voltage as can be seen in Fig. 6. As was previously

stressed, a higher voltage means lower concentrations of free carriers and thus a lower trapping probability. Also, at higher voltages a larger increase of space charge is needed to introduce an undepleted region into the device.

The rate of the TCT signal decay is also a function of laser pulse frequency. However at a laser repetition rate of 1Hz, the rate used in these measurements, surface generation is completely dominated by laser diode bleeding. The laser bleeding (in general case negligible emission of light from the laser diode when it is in the off mode) was carefully evaluated by means of a photomultiplier (Philips 2020Q) and timing analysis to have the power of 3 pW. Therefore the flux of 1×10^7 photons/s resulting from laser bleeding dominated the flux of 5×10^5 photons/s from the 1 Hz laser pulse.

The time decay of the TCT signal, on the other hand, showed no correlation with the time the diode was kept under bias. A delay of up to 300 s was introduced between the time of applying the bias to the diode and the time of starting the laser. No degradation of the TCT signal as a function of this delay was observed on the time scale of our measurements. This leads to the conclusion that the time decay of the TCT signal is caused by surface generation and not by the leakage current. These observations are in agreement with the results reported in [8].

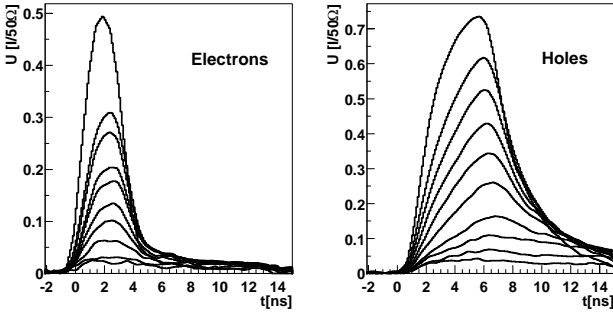


Fig. 7. Electron injection and hole injection waveforms at different values of signal integral. The highest waveform was measured at $t=0$ after starting the measurement. The subsequent waveforms were obtained at later times as the signal integral decayed ($w3394$, $\phi_{\text{eq}}=2 \times 10^{14}$ n/cm², $T = 83$ K, $U_b = 100$ V).

In Fig. 7 signal shapes are shown at different times after starting the measurement for electrons and holes. Although the signals at this temperature are too fast and too close to the resolution of the system to draw a definitive conclusion, one could suggest that at $t = 0$ the signals are of high field injection type for electrons and low-field injection type for holes, which means that the diode is of n-bulk type at this temperature. The waveforms in Fig. 7 indicate that at later times the transition from n to p type might have occurred in the case of electrons, whereas in the case of holes the field strength on the injection side decreased (i.e. the amount of positive space charge increased).

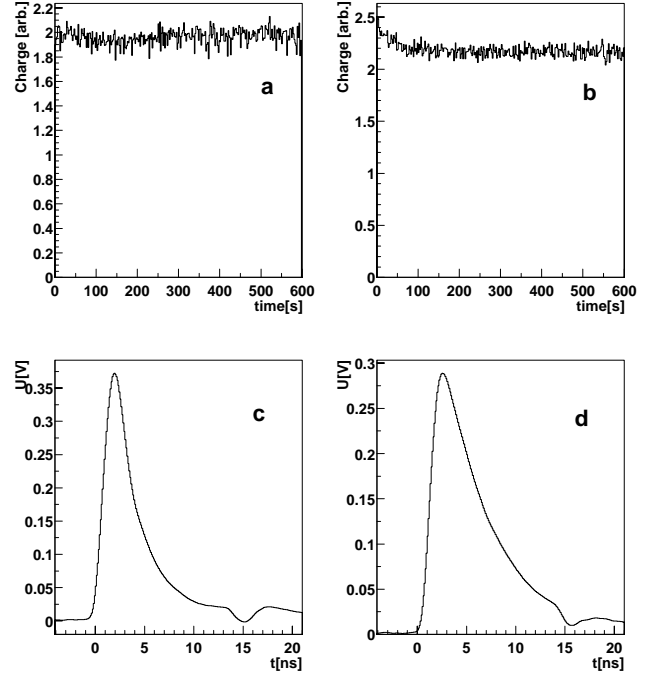


Fig. 8. Time dependence of electron a) and hole b) signal integrals. Electron c) and hole d) signal shapes averaged from $t = 300$ s to $t = 400$ s. ($w3394$, $\phi_{\text{eq}} = 2 \times 10^{14}$ n/cm², $T = 83$ K, $U_b = 100$ V, opposite side illumination)

If the time decay of the TCT signal is to be explained by trapping of the charge induced by the pulsed laser, then the continuous injection of opposite sign charge would have to compensate for the effect, causing the time dependence to disappear. This can be nicely seen in Fig. 8 showing the TCT signals for electrons and holes while the other side of the diode was illuminated with DC red light laser. The DC light was of much higher intensity than the light of the laser pulses. One can see that in both cases the signals are of high field injection type and that the signal does not decay with time. An attempt to illuminate the same side of the detector results in immediate decay of the TCT signal, as could be expected from the results presented here.

IV. CONCLUSIONS

It was shown that close to room temperature continuous carrier injection in Si detectors irradiated beyond charge inversion causes charge trapping thus affecting the N_{eff} . The increased negative space charge caused by electron injection degrades detector performance. Hole injection, on the other hand, compensates for the charge stored in deep level defects. The result is type re-inversion from p^+-p-n^+ back to p^+-n-n^+ . By choosing an appropriate injection level at a given temperature the minimum FDV can be reached. In this so-called ideal working point, the change in FDV as a function of irradiation fluence is surprisingly small.

At cryogenic temperatures similar behavior with a different manifestation can be observed. The signal decay with time can be explained by trapping of the charge induced by the

laser light. Due to very long detrapping times at low temperatures this trapped charge changes the space charge so that the diode becomes undepleted. In addition the sign of the trapped charge is such that the junction moves away from the light injection side. Again time decay can be eliminated by continuously injecting charges of opposite sign from the back plane of the detector.

V. ACKNOWLEDGEMENTS

The authors would like to express gratitude to the ROSE collaboration, especially to dr. M Moll, for providing STM samples. We would also like to thank Erik Margan for his brilliant technical solutions and helpful discussions during construction of the TCT set-up.

VI. REFERENCES

- [1] G. Lutz, "Effects of Deep Level Defects in Semiconductor Detectors," Nucl. Instr. Meth., vol. A377, pp. 234-243, 1996.
- [2] V. Eremin and E. Verbitskaja, "Analytical Simulation of Electric Field Manipulation and Reduction of Full Depletion Voltage by Non-Equilibrium Carrier Injection", pres. at RD39 workshop, unpublished.
- [3] B. Dezille, V. Eremin and Z. Li, "Improved Radiation Hardness for Si detectors," IEEE Trans. Nucl. Sci, vol. 46, No. 3, pp. 221-227, 1999.
- [4] W.C. Dash and R. Newman, "Intrinsic Optical Absorption in Single Cristal Germanium and Silicon at 77K and 300K," Phys. Rev., no. 99, pp . 1151, 1955.
- [5] H. Feick., "Radiation Tolerance of Silicon Particle Detectors for High-Energy Physics Experiments," Doctoral thesis, DESY Internal Report, DESY F35D-97-08, 1997.
- [6] G. Kramberger, V. Cindro, I. Mandic, M. Mikuz and M. Zavrtanik, "Determination of effective trapping times for electron and holes in irradiated silicon," Nucl. Instr. Meth., submitted for publication.
- [7] K. Boer, S. Janos, V.G. Palmieri, B. Dezillie, Z. Li, P. Collins, et. al., "Charge Collection Efficiency of Irradiated Silicon Detector Operated at Cryogenic Temperatures," Nucl. Instr. Meth., vol. A440, pp. 5-16, 2000.
- [8] B. Dezillie, V Eremin, Z. Li, and E. Verbitskaya, "Polarization of Silicon Detectors by Minimum ionizing Particles", Nucl. Instr. Meth., A452, pp. 440-453, 2000.